scientific reports

Check for updates

OPEN

Mobility constraints in segregation models

Daniele Gambetta[1,2]✉, Giovanni Mauro[1,2,3]✉ & Luca Pappalardo[1]✉

Since the development of the original Schelling model of urban segregation, several enhancements have been proposed, but none have considered the impact of mobility constraints on model dynamics. Recent studies have shown that human mobility follows specific patterns, such as a preference for short distances and dense locations. This paper proposes a segregation model incorporating mobility constraints to make agents select their location based on distance and location relevance. Our findings indicate that the mobility-constrained model produces lower segregation levels but takes longer to converge than the original Schelling model. We identified a few persistently unhappy agents from the minority group who cause this prolonged convergence time and lower segregation level as they move around the grid centre. Our study presents a more realistic representation of how agents move in urban areas and provides a novel and insightful approach to analyzing the impact of mobility constraints on segregation models. We highlight the significance of incorporating mobility constraints when policymakers design interventions to address urban segregation.

Understanding urban segregation, which refers to the spatial separation and concentration of different social groups within an urban area, is of paramount importance given its impact on various social, economic, and cultural facets of our society[1–4]. For example, high levels of segregation lead to limited access to quality education, healthcare, and employment opportunities for marginalized communities, exacerbating socioeconomic disparities and hindering social mobility[5–7]. Additionally, concentrated poverty resulting from segregation strain public resources, contribute to higher crime rates, and foster social isolation, further impeding community development and cohesion[8,9]. Particularly crucial is the mathematical modelling of the mechanisms underlying segregation dynamics, as it provides a robust tool for conducting insightful what-if analyses, understanding the intricacies of social inequities, facilitating integration, and promoting social cohesion[2,10]. Thus, it is unsurprising that modelling urban segregation has attracted the attention and efforts of scientists from different disciplines[11–19].

In 1971, economist Thomas Schelling proposed an agent-based model to explain how individual actions could result in global phenomena, focusing on urban segregation[20–23]. He observed that segregation dynamics emerge due to homophily among social groups across various demographic factors such as ethnicity, language, income, and class affiliation[23]. To illustrate this idea, Schelling used a simple spatial proximity model that divided the population into two groups based on a homophily threshold. Agents of two colours were placed randomly on a two-dimensional grid, and each agent preferred to live next to people in their group. If an agent is unhappy with their current location, they will move to the nearest square that satisfies them. Schelling found that segregation emerges above a homophily threshold of 1/3, and other factors affecting segregation include the ratio of individuals, the homophily threshold, and individual demands.

Numerous variants and enhancements of the Schelling model have been proposed so far, modifying agents' behaviour[11–13], environmental configuration[24–29], considering geographical regions[14–16], including real-world segregation data along with strategies to validate simulated behaviour with observations[17–19], implementing agent behaviours based on psychological and sociological theories[30–33], and allowing for sensitivity analysis to quantify outcome dependency on various parameters and initial conditions[10,34–36]. Other works show how even milder preferences or integration policies can eventually lead to unexpected segregation scenarios[37,38], and how the introduction of venues can have an impact on segregation dynamics[39].

Despite these advancements, all proposed models assume that unhappy agents move randomly on the grid without any preference for nearby or far away locations. However, recent empirical studies have shown that human movement, far from being random, follows specific statistical patterns across various spatial scales, including daily movements and migrations[40–53]. These individual mobility patterns are characterized by a preference for short distances and relevant places over longer distances and sparse ones[40–45,48,54–57]. Despite considerable interest in modelling and predicting human mobility[43,52], it remains unclear how mobility patterns relate to

[1]Institute of Information Science and Technologies, National Research Council (ISTI-CNR), Pisa, Italy. [2]University of Pisa, Pisa, Italy. [3]IMT School for Advanced Studies, Lucca, Italy. ✉email: daniele.gambetta@phd.unipi.it; giovanni.mauro@phd.unipi.it; luca.pappalardo@isti.cnr.it

segregation patterns. Recent empirical studies suggest a link between experienced income segregation and an individual's tendency to explore new places and visitors from different income groups[58], but this has not been systematically studied in an agent-based, Schelling-like simulation framework. At the same time, although a few simulation studies show how restricting relocation options[25] and considering collective factors[33,59] affect segregation dynamics, these findings have not been related to mobility constraints. Thus, we still lack a comprehensive understanding of how mobility constraints impact segregation dynamics.

This study fills this gap by designing a segregation model that considers mobility constraints and exploring how they influence segregation dynamics. Drawing on the gravity law of human mobility[48,55,60–63], our model allows unhappy agents to select the next location to move based on distance and location relevance. Our findings reveal that mobility-constrained models exhibit lower levels of segregation than the Schelling model, albeit with a longer convergence time, and that agents that end in the periphery are more segregated than those in the grid centre. We attribute these phenomena to a small group of persistently unhappy agents from the minority group who gravitate towards the grid centre due to the preference for nearby and relevant locations imposed by mobility constraints.

Mobility-constrained segregation models

In our model, agents may be of two types, moving on a bi-dimensional grid of size $m = N \times N$. As in the original Schelling model[20–23], an agent is happy when it is surrounded by a number of agents of the same type above a predetermined homophily threshold. An unhappy agent located at a cell A moves to a new cell B based on a probability function, $p(B)$, which depends on two factors: the distance $d(A, B)$ between A and B, and the relevance $r(B)$ of destination B. This probability captures the gravity law of human mobility[43,47,48,52,55,60–64], positing that people tend to travel to nearby and relevant locations, a concept that has been supported by extensive research in fields ranging from transport planning[65] and spatial economics[62,66,67] to epidemic spreading[57,68–71]. The distance between points A and B, represented by coordinates (x_A, y_A) and (x_B, y_B), is computed as their Euclidean distance on the grid, $d(A, B) = \sqrt{(x_A - x_B)^2 + (y_A - y_B)^2}$. Mathematically, we define the probability of an agent moving to cell B, given its current cell A, as a product of two power-law functions:

$$p(B) \propto r(B)^{\alpha} d(A, B)^{\beta} \tag{1}$$

where parameter $\alpha > 0$ models the tendency to move preferably to relevant places, while β captures the tendency to prefer ($\beta > 0$) or avoid ($\beta < 0$) large displacements. These two parameters govern the influence of distance and relevance on the simulation outcomes, encapsulating the essential factors that shape the dynamics of the model.

We assume a core-periphery structure to model the distribution of relevance across the grid cells[72] and use a radial distribution where the relevance value of each cell decreases with its distance from the grid centre C:

$$r(A) \propto \frac{1}{d(A, C)^{\kappa}} \tag{2}$$

with $\kappa = 2$. The results obtained with a uniformly random spatial distribution of relevance can be found in Supplementary Note 1. Note that since all agents share the information about cell relevance, $\alpha = -x$ means being repelled by a cell to the same extent that $\alpha = x$ means being attracted to it. The case where $\alpha = 0$ and $\beta = 0$ corresponds to the original Schelling model. The model simulation ends when all agents are happy. From the gravity segregation model, we derive two other families of models: the distance models ($\alpha = 0, \beta \neq 0$), which only imposes constraints on distance, and the relevance models ($\alpha \neq 0, \beta = 0$), which only considers relevance. See Table 1 for algorithmic details about the gravity, relevance, and distance models.

We conduct a series of experiments varying the grid size ($m \in \{25 \times 25, 50 \times 50, 75 \times 75\}$), the ratio of occupied cells ($\sigma \in \{50\%, 70\%\}$), the proportion of agents in the two groups ($\theta = \{10/90, 30/70, 50/50\}$), the homophily threshold ($h \in \{10\%, 30\%, 50\%\}$), and the relocation policy (whether agents move to locations where they should be happy or not). Since our results are consistent across these different parameter values (see Supplementary Note 2), we present the findings for a fixed set of conditions: a grid size of 50×50, an occupancy ratio of 70%, a group proportion of 30/70, and a homophily threshold of 30%. We perform 100 simulations for each set of parameter values, each time using a different random distribution of agents on the grid. Each simulation terminates when all agents are happy or after a maximum of 500 simulation steps.

We quantify the level of segregation at the end of the simulation as the average segregation level of the agents, $S = \frac{\sum_{a \in M} s(a)}{|M|}$, where M is the set of agents and $s(a) = \frac{|\Gamma_T(a)|}{|\Gamma(a)|}$, with $\Gamma_T(a)$ the set of neighbours of the same type of a and $\Gamma(a)$ the set of neighbours of a of any type. $\Gamma_T(a)$ is computed as the Moore neighbourhood with range $r = 1$[73]. We obtain analogous results when using other segregation metrics (see Supplementary Note 3).

Results

The values of parameters α and β influence how agents move on the grid when unhappy, generating different mobility patterns. As an example, in Fig. 1, we compare three simulations with identical initial configuration but different parameter values: $\alpha = \beta = 0$, representing the original Schelling model O; $\alpha = 0, \beta = -2$, a distance model D; $\alpha = 2, \beta = 0$, a relevance model R; and $\alpha = 2, \beta = -2$, a gravity model G. In the original Schelling model (O), agents move randomly throughout the grid when they are unhappy, resulting in a distribution of jump lengths that follows a peaked distribution, indicating the existence of a typical jump length for agents ($\overline{d_O} = 16.27$, the average distance between cells on the grid). On the other hand, in the distance model (D) and the gravity model (G), agents prefer to move to nearby cells, resulting in a heavy-tailed distribution of jump

	Distance	Relevance	Gravity
Initialization			
Agents randomly assigned to a group based on θ and placed randomly on the grid based on σ. $\forall$ cell A, relevance $r(A)$ assigned as:	$r(A) = 1$	$r(A) \propto \frac{1}{d(A,C)^2}$, where C is the grid's centre and $d(A, C)$ indicates the distance between A and C.	$r(A) \propto \frac{1}{d(A,C)^2}$, where C is the grid's centre and $d(A, C)$ indicates the distance between A and C.
Simulation step			
Unhappy agents move to an empty cell B on the grid with probability:	$P(B) = d(A, B)^{\beta}$	$P(B) = r(B)^{\alpha}$	$P(B) = r(B)^{\alpha} d(A, B)^{\beta}$
Termination			
When all the agents are happy, or after a maximum of 500 simulation steps.			

Table 1. Schema of the distance, relevance, and gravity models. Each model has three phases: Initialization, Simulation Step, and Termination. In the Initialization phase, the Relevance and Gravity models assign a core-periphery relevance to the cells inversely proportional to their distance from the centre of the grid C. The Distance model assigns a uniform relevance to all cells. During the Simulation Step, when an agent in cell A needs to relocate, the probability of choosing a cell B for relocation depends on the model being used. In the Distance model, this probability is proportional to the distance between cell A and cell B. In the Relevance model, the probability is proportional to the relevance of cell B. In the Gravity model, the probability is proportional to the product of the distance and the relevance of cell B. These probabilistic rules govern the relocation decisions of agents in the respective models, determining their movements within the grid. The Termination phase marks the end of the simulation when all agents are happy or a maximum of 500 simulation steps is reached.

lengths (Fig. 1j,k) and lower average distances ($\overline{d_D} = 5.30$ and $\overline{d_G} = 3.10$). In R and G, agents are directed towards the city centre, resulting in a lower average distance travelled ($\overline{d_R} = 11.60$) than O and a centripetal tendency that causes the empty cells to be positioned far away from the centre of the grid (Fig. 1c,d). Indeed, in R and G, only 4% and 7% of the cells in the centre are empty, while in D and O, 25% and 28% of cells are empty, respectively. An intriguing question is what impact α and β, and thus the resulting mobility patterns, have on crucial aspects of the simulation, such as the final segregation level, S, and model convergence time, n, defined as the number of simulation steps needed for all the agents to become happy.

Effects of distance on segregation dynamics. We study the impact of varying the distance exponent β on the final level of segregation S and the convergence time n while holding the relevance parameter constant ($\alpha = 0$).

Figure 2a displays the relationship between n and S for $\beta \in [-5, 5]$. In the figure, we present only the average values of S and n over 100 simulations since the standard deviation is relatively small (see Supplementary Note 4). We find that a decrease in β (i.e., an increasing cost of relocating far away) leads to a decrease in S and a increase in n compared to the original Schelling model ($\beta = 0$). This result means that a preference to move nearby the current location slows down but mitigates the segregation behaviour. For instance, for $\beta = -5$, S is reduced by around 10%, and n increases by a factor of 30 compared to the original Schelling model ($\beta = 0$). Conversely, an increase in β (lower cost of relocating far) has a negligible impact on n and marginally increases S. Indeed, for $\beta = 5$, the segregation level increases only by around 1% compared to the original Schelling model, with no substantial change in the convergence time. As an example, Fig. 1a-d presents the final grid configurations for O, R, D, and G: note how D and G (with $\beta = -2$), which converge over a longer time, have a lower final segregation level compared to O and R.

We also observe that β influences n and S in a non-linear fashion. The dependency of n and β, can be approximated by an exponential function:

$$n = a^{-b\beta} + c \tag{3}$$

with $a = 2.7, b = 1.1, c = 21$ (Fig. 2b). Equation 3 enables us to estimate the number of simulation steps required for the model to converge based solely on the value of β, providing valuable what-if insights into the implications of mobility constraints on segregation dynamics. For example, if an incentive for relocating far away from the current location is introduced, which would result in a positive value of β (e.g., $\beta = 5$), Eq. (3) suggests that it would take approximately $n = 21$ simulation steps for the city to become segregated. On the other hand, if people are incentivised to stay nearby the current location, which would result in a negative value of β (e.g., $\beta = -5$), Eq. (3) suggests that an average of $n = 256$ simulation steps (more than ten times more) would be required for the city to become segregated.

The relationship between β and S is well-fitted by a sigmoid function:

$$S = \frac{a}{d^{-b\beta} + c} + k \tag{4}$$

where $a = 8.5 \times 10^{-1}, b = 3.2, c = 11.8, d = 1.4, k = 7.3 \times 10^{-1}$ have been empirically fitted (Fig. 2c). An interesting finding is a tipping point in the sigmoid curve close to $\beta = 0$ (original Schelling model), which indicates that the influence of β on the level of segregation depends on whether it is positive or negative (Fig. 2c). When

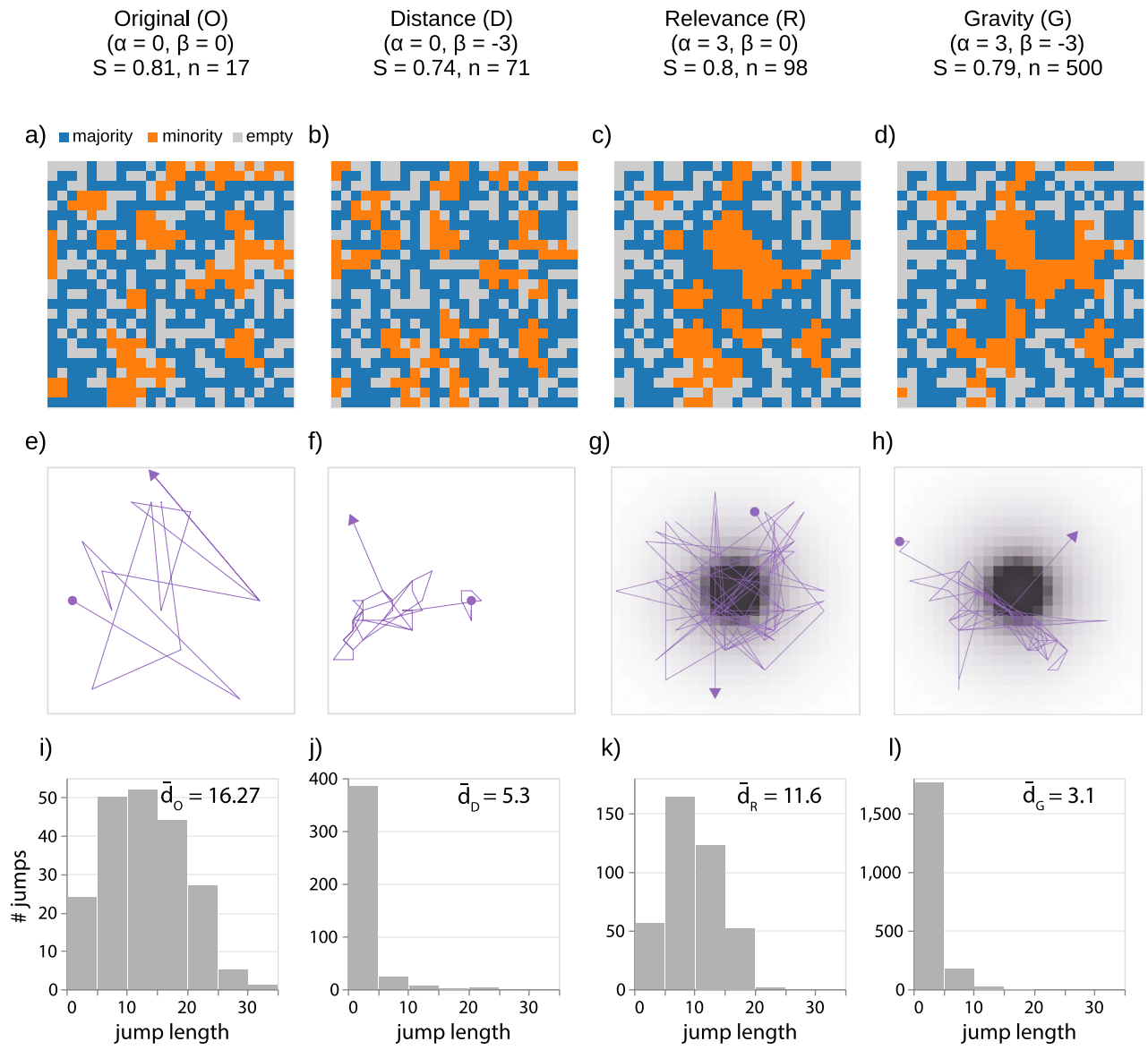

Figure 1. Segregation dynamics of mobility-constrained models. (**a**–**d**) Final grid configuration of four simulations of the original Schelling model *O* (**a**), a distance model *D* (**b**), a relevance model *R* (**c**), and a gravity model *G* (**d**), all with a grid size of 25 × 25, a cell occupancy rate of 70%, a group proportion of 30/70, and a homophily threshold of 30%. (**e**–**h**) The mobility trajectories of four agents, one per model. (**i**–**l**) Graphical representation of the distribution of jump length for each model. In *O*, agents move randomly throughout the grid when they are unhappy, resulting in a peaked distribution of jump lengths. In *D* and *G*, agents prefer to move to nearby cells, resulting in a heavy-tailed distribution of jump lengths. In *R* and *G*, agents are directed towards the city centre, resulting in a centripetal tendency that causes empty cells to be positioned far away from the centre and a lower average distance travelled than *O*. We indicate the average distance travelled by agents in the four models with $\bar{d}_O$, $\bar{d}_D$, $\bar{d}_R$, and $\bar{d}_G$.

$\beta > 0$, agents move far way over a larger pool of choices because the number of available cells increases with distance, leading to behaviour that closely resembles the original Schelling model (see Fig. 2a). In fact, even for $\beta = 5$, the final segregation level S is only 1% higher than the original Schelling model (Fig. 2c). In contrast, when $\beta < 0$, agents prefer to stay close to their current cells, causing the grid configuration to change slowly over time and leading to a final grid configuration that is more similar to the initial one (and therefore less segregated). For example, if $\beta = -5$, the segregation level $S = 0.73$, about 8% lower than the original Schelling model.

The relation between S and n is well-fitted by a power-law function:

$$S = \frac{a}{n^b} + c \tag{5}$$

with $a = 4.6$, $b = 1.5$, and $c = 0.7$ (Fig. 2a). As n increases, the overall level of segregation S decreases: the more difficult it is for the agents to find cells that meet their homophily preferences, the less segregated the final grid

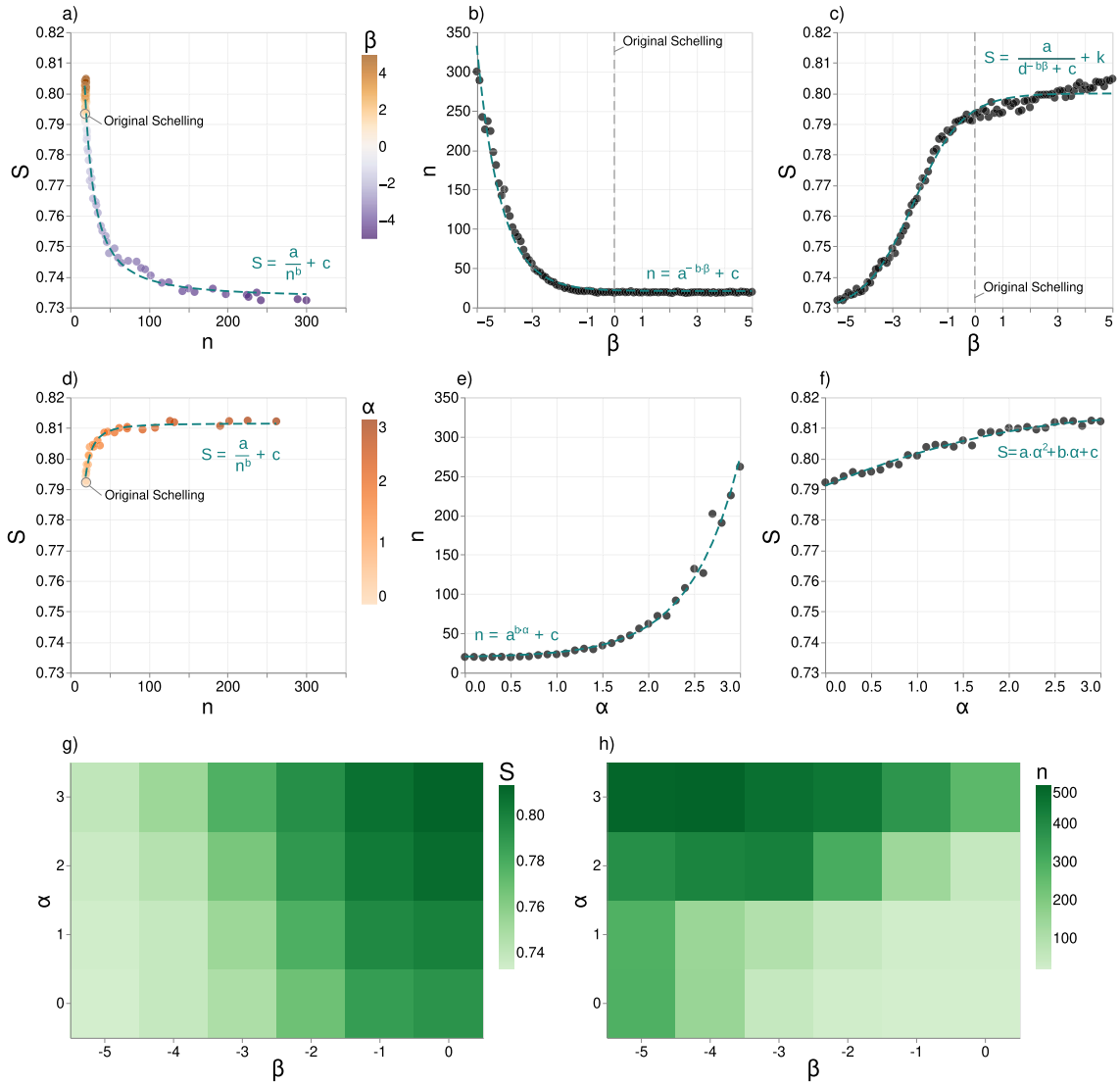

Figure 2. Effects of distance and relevance on segregation dynamics. (**a**–**c**) Effects of β on segregation dynamics. (**a**) The average value of n and S over 100 simulations with the same β value but different initial grid configurations, colour-coded by the value of β. The lower β, the higher the cost of relocating far away, resulting in longer convergence time and reduced segregation levels compared to the original Schelling model. The relationship between n and S is well fitted by a power-law function $S = \frac{a}{n^b} + c$, with $a = 4.6, b = 1.5, c = 0.7$. (**b**) β vs average n over 100 simulations. The relationship follows an exponential distribution $n = a^{-b\beta} + c$, with $a = 2.7, b = 1.1, c = 21.0$. The lower β (< 0), the longer the simulation. (**c**) β vs average S over 100 simulations. This is well approximated by a sigmoid function $S = \frac{a}{d^{-b\beta}+c} + k$, with $a = 0.9, b = 3.2, c = 11.8, d = 1.4, k = 0.7$ For $\beta < 0$, there is an exponential increase in S; $\beta > 0$, the growth is moderate. (**d**–**f**) Effects of α on segregation dynamics. (**d**) The average value of n and S over 100 simulations with the same value of α but different initial grid configurations, colour-coded by the value of α. Increasing values of α elongate n and slightly increase S. The relationship follows a power-law function $S = \frac{a}{n^b} + c$, with $a = -8.5, b = 2.1, c = 0.8$. (**e**) α vs average n over 100 simulations. The relationship follows an exponential distribution $n = a^{b\alpha} + c$, with $a = 7.1, b = 0.9, c = 19.5$. (**f**) α vs average S over 100 simulations. The relationship is well approximated by a parabolic function $S = a\alpha^2 + b\alpha + c$, with $a = -0.002, b = 0.01, c = 0.8$. (**g**) The average S (colour) for each combination of α and $\beta < 0$. For every value of α, higher β values lead to a higher S; for every β, higher α values lead to a higher S. (**h**) The average n (colour) for each combination of α and $\beta < 0$. For every value of α, higher β values lead to a lower n; for every β, higher α values lead to higher n.

is, and the more steps are required to reach an equilibrium state where all agents are happy. Conversely, if the agents can quickly identify desirable locations, convergence occurs rapidly with fewer steps, resulting in greater segregation.

Effects of relevance on segregation dynamics. We study the impact of the relevance exponent α on the final level of segregation S and the convergence time n by controlling for the distance parameter ($\beta = 0$). We find that n increases exponentially with α as:

$$n = a^{b \cdot \alpha} + c \tag{6}$$

where $a = 7.1, b = 0.94$, and $c = 19.5$ are empirically fitted (Fig. 2e). This result suggests that agents tend to move closer to the opposing group when they compete for relevant cells, resulting in a more prolonged convergence process than the original Schelling model. For example, $\alpha = 3$ corresponds to an average of 261 simulation steps, almost 12 times more than the needed for $\alpha = 0$ (20 steps on average). On the other hand, S increases parabolically with α as:

$$S = a \cdot \alpha^2 + b \cdot \alpha + c \tag{7}$$

where $a = -0.002, b = 0.01, c = 0.8$ empirically fitted (Fig. 2f), indicating a slightly non-linear impact of α on the final segregation level. When $\alpha = 3, S = 0.81$, a mere 2.5% higher than the original Schelling model (0.79), indicating that the relevance parameter has only a minor effect on the final segregation level.

The relationship between n and S through the relevance exponent α can be approximated by power-law function:

$$S = \frac{a}{n^b} + c \tag{8}$$

with $a = -8.5, b = 2.1, c = 0.8$ (Fig. 2d). The longer it takes for the model to converge (larger n), the more segregated the final grid becomes (higher S, albeit only slightly). We observe that as α increases, the difference in segregation levels between the periphery and centre, denoted as $S_{\text{diff}} = S_{\text{periphery}} - S_{\text{centre}}$, also increases. This means that agents that end up in the periphery are more segregated than those in the centre (see Supplementary Note 5). This can be attributed to the centripetal force that encourages agents to move towards the centre, creating a more mixed scenario than in the periphery. Since the periphery is larger and shows a higher segregation level than the centre, the final grid becomes more segregated (higher S) as α increases.

Interplay of distance and relevance. Finally, we study the interplay of the relevance and distance exponents on segregation dynamics. We focus on the negative values of β, which induce the most significant variations in S and n. For completeness, we provide an analysis of $\beta > 0$ in Supplementary Note 6.

Segregation is maximized in the relevance model ($\beta = 0$) and minimized when $\beta = -5$, with a minor influence of parameter α (Fig. 2g). Specifically, $S_{\beta=0,\alpha=3}$ is approximately 11% higher than $S_{\beta=-5,\alpha=0}$. This suggests that when the preference for short distances is strong, the impact of relevance is relatively weak. Figure 2h shows that the convergence time is maximized when β is low and α is high (upper left corner). In particular, $n_{\beta=-5,\alpha=3}$ is roughly 24 times higher than $n_{\beta=0,\alpha=0}$. Distance constraints become almost irrelevant when relevant places are present in influencing convergence time. Overall, our results highlight the complexity of the interplay between β and α and their differential impacts on segregation level and convergence time.

One intriguing aspect is the identification of agents responsible for elongating convergence time in the gravity models. Do all agents suffer prolonged unhappiness, or is there a specific group of agents responsible for the extended convergence time? Figure 3a–b illustrates the distribution of time-to-happiness, representing the number of simulation steps needed for agents to become happy. Our results indicate that most agents achieve happiness within a few steps, while a small fraction of agents, primarily from the minority group, remain unhappy for an extended duration. For example, as Fig. 3a shows, all agents of the majority group achieve happiness within 17 simulation steps. In contrast, although most minority group agents attain happiness relatively quickly, some remain unhappy for an extended period for up to 500 simulation steps (Fig. 3b). We classify these agents as persistently unhappy and denote them as set U. Specifically, we identify persistently unhappy agents as those whose unhappiness surpasses the 95th percentile of the distribution of time-to-happiness for all agents. For example, in Fig. 3c, only 9 agents out of 1750 are persistently unhappy.

We hypothesize that the combination of agents' preferences and the distribution of relevant cells within the grid creates a situation where some agents may be trapped in an area that does not align with their preferences, resulting in persistent unhappiness. We discover that this area is a "suburbia" of the centre, i.e., an area around the centre between a radius of 9 and a radius of 16.6, representing 25% of the grid's total area (see Fig. 3c). In detail, we compute the fraction ρ of persistently unhappy agents being located in the suburbia at a critical point when the centre becomes stably segregated (see Supplementary Note 7). For instance, Fig. 3c illustrates the grid configuration of a gravity model at this critical point: the majority of persistently unhappy agents (white dots) are concentrated in a confined region near the centre of the grid. Mathematically, we capture this aspect by defining $\rho = \frac{|U_{sub}|}{|U|}$, where $|U_{sub}|$ is the number of persistently unhappy agents in the suburbia at the critical point. Figure 3d shows that the gravity and the relevance models have a significantly higher ρ than a random spatial distribution of agents, with the relevance model displaying a lower probability than the gravity model. The distance model's probability is instead similar to the null model. These findings suggest that persistently unhappy agents are located in suburbia at the critical point, and their presence can significantly prolong the simulation

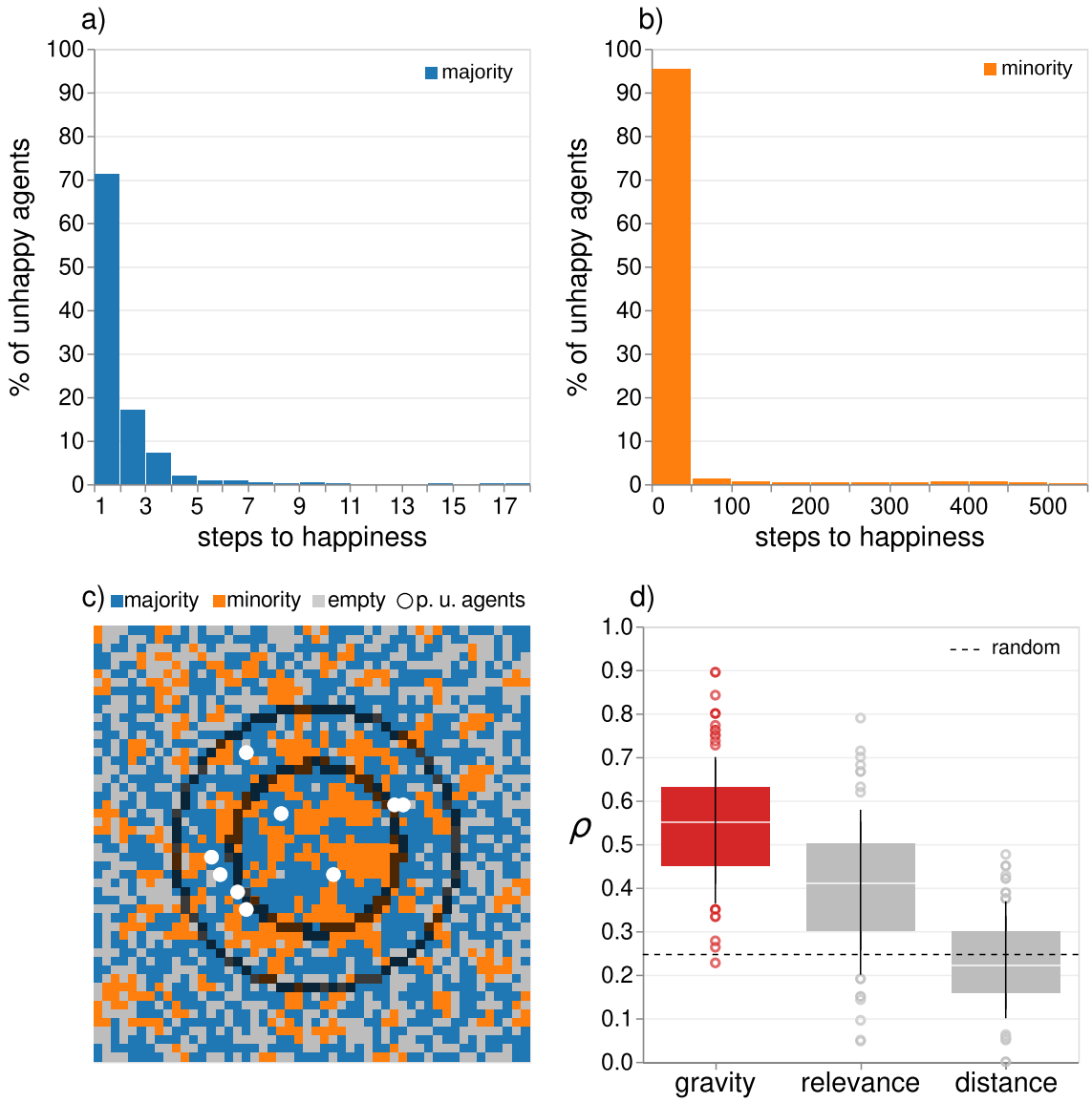

Figure 3. Persistently unhappy agents. (**a**) Distribution of simulation steps required for the agents in the majority group to achieve happiness (100 simulations of the gravity model, $\alpha = 3, \beta = -3$). All agents reach happiness within 17 steps. (**b**) Distribution of simulation steps needed for agents in the minority group to reach happiness. Most agents become happy in 50 steps, but a small percentage remain unhappy for up to 500 steps. (**c**) Gravity model's grid configuration at the critical point when the centre becomes stably segregated. The boundaries of the suburbia are represented as two dark circles with a radius of 9 (small circle) and 16.6 (large circle), representing 25% of the grid's total area. The white dots represent persistently unhappy agents who remain unhappy for more than the 95th percentile of simulation steps. Most of these agents are in the suburbia region. (**d**) Probability ρ of a persistently unhappy agent being in suburbia at the critical point when the centre becomes stably segregated. The dashed line indicates the probability of a random agent being in the area (0.25). The gravity and relevance models show higher probabilities than the random model, while the distance model's probability is similar to the null model.

as they cannot escape the loosely segregated situation in the centre due to their preference for relevant locations and short-distance moves.

Discussion

This study provides a novel and insightful approach to understanding the impact of mobility constraints on urban segregation dynamics. The gravity law injected in the Schelling model allows for modelling agents' mobility patterns based on the relevance of locations and the distance between them. We find that the influence of these two factors on segregation dynamics is significant and profoundly impacts the model outcome, both independently or in combination with each other. By analyzing the mobility patterns of agents in the gravity-constrained model, we discovered a trend in the exponential elongation of segregating times attributed to a few agents of the

minority group caught in a vicious loop, constantly moving among the few locations near the segregated centre. Moreover, the centripetal force towards the centre leads to more mixing in the centre and greater segregation in the periphery.

Our findings provide valuable insights into the complex dynamics of segregation, offering a valuable tool for understanding and simulating potential scenarios through what-if analysis. The equations that relate the relevance and distance parameters with the segregation level and the convergence time can be manipulated to explore different scenarios, such as economic incentives to encourage large-scale relocations or the relocation of facilities within a city. This approach can provide policymakers with a comprehensive understanding of how these interventions may impact segregation dynamics.

It is worth noting that, in recent years, a few studies have explored the relationship between agents' freedom to move and segregation dynamics. Notably, Fagiolo et al.[25] examined the consequences of agents' restricted movement to specific nodes within a network, Abella et al.[33] explored the impact of agents developing attachments to particular places as they spent time there, and Moro et al.[58] shed light on the association between experienced income segregation and place and social exploration. However, none of these studies has thoroughly examined, within a what-if analysis, the profound effects on segregation dynamics of geographic distance, location relevance, and their interplay. Our study addresses this gap by unveiling this impact on the segregation level and model's convergence time for the first time.

While our study provides valuable insights, it has limitations and areas for further exploration. Our model's reliance on simplified assumptions, including a grid-like structure with core-periphery relevance distribution and agents' satisfaction based solely on neighbour tolerance, overlooks other factors contributing to overall happiness. Future research could incorporate more complex assumptions and consider additional factors such as socio-economic status, housing conditions, and neighbourhood composition. For example, when making relocation decisions, agents could consider several attributes of origin and destination cells, such as cell centrality and the presence of specific venues[43,48], allowing for a more comprehensive assessment of happiness based on multiple factors, rather than solely relying on group homophily. In addition, there is potential for exploring alternative mechanisms of agent mobility. For instance, to capture individual mobility patterns more realistically, we could assign individual mobility networks to agents[56,74], limiting their movement to specific subsets of cells on the grid. Lastly, we aim to extend the analysis to a real-world dataset of relocations to assess how simulation-based results align with empirical observations in an actual city.

Data availability

All data generated during this study are included in this published article and its supplementary information files and can be found in the code repository available at https://github.com/dgambit/mobility_schelling. The study does not involve any human participants.

Code availability

Code availability The Python code to replicate the models and all the experiments is available at https://github.com/dgambit/mobility_schelling.

Received: 17 May 2023; Accepted: 10 July 2023
Published online: 26 July 2023

References

1. Orfield, G. & Lee, C. *Why Segregation Matters: Poverty and Educational Inequality* (Civil Rights Project at Harvard University, 2005).
2. Langellier, B. A. An agent-based simulation of persistent inequalities in health behavior: Understanding the interdependent roles of segregation, clustering, and social influence. *SSM Popul. Health* **2**, 757–769 (2016).
3. Jan Nijman, Y. D. W. Urban inequalities in the 21st century economy. *Appl. Geogr.* **117**, 1–10 (2020).
4. Crowell, A. & Fossett, M. Metropolitan racial residential segregation in the united states. *Demogr. Res.* **46**, 217–260 (2022).
5. Locke, D. H. *et al.* Residential housing segregation and urban tree canopy in 37 us cities. *NPJ Urban Sustain.* **1**, 15 (2021).
6. Fogli, A. & Guerrieri, V. *The End of the American Dream? Inequality and Segregation in US Cities* (National Bureau of Economic Research, 2019).
7. Kodros, J. K. *et al.* Unequal airborne exposure to toxic metals associated with race, ethnicity, and segregation in the USA. *Nat. Commun.* **13**, 6329 (2022).
8. Logan, J. R. & Messner, S. F. Racial residential segregation and suburban violent crime. *Soc. Sci. Q.* **68**, 510 (1987).
9. Krivo, L. J., Peterson, R. D. & Kuhl, D. C. Segregation, racial structure, and neighborhood violent crime. *Am. J. Sociol.* **114**, 1765–1802 (2009).
10. Clark, W. A. & Fossett, M. Understanding the social context of the Schelling segregation model. *Proc. Natl. Acad. Sci.* **105**, 4109–4114 (2008).
11. Laurie, A. J. & Jaggi, N. K. Role of 'vision' in neighbourhood racial segregation: A variant of the Schelling segregation model. *Urban Stud.* **40**, 2687–2704 (2003).
12. Mantzaris, A. V. Incorporating a monetary variable into the Schelling model addresses the issue of a decreasing entropy trace. *Sci. Rep.* **10**, 17005 (2020).
13. Sert, E., Bar-Yam, Y. & Morales, A. J. Segregation dynamics with reinforcement learning and agent based modeling. *Sci. Rep.* **10**, 11771 (2020).
14. Gimblett, H. R. *Integrating Geographic Information Systems and Agent-Based Modeling Techniques for Simulating Social and Ecological Processes* (Oxford University Press, 2002).
15. Benenson, I. & Torrens, P. *Geosimulation: Automata-Based Modeling of Urban Phenomena* (Wiley, 2004).
16. Benenson, I., Omer, I. & Hatna, E. Entity-based modeling of urban residential dynamics: The case of Yaffo, Tel Aviv. *Environ. Plann. B* **29**, 491–512 (2002).
17. Park, B. H., Aziz, H. A., Morton, A. & Stewart, R. High performance data driven agent-based modeling framework for simulation of commute mode choices in metropolitan area. in *2018 21st International Conference on Intelligent Transportation Systems (ITSC)*, 3779–3784 (IEEE, 2018).

18. Venkatramanan, S. *et al.* Using data-driven agent-based models for forecasting emerging infectious diseases. *Epidemics* **22**, 43–49 (2018).
19. Zhang, H., Vorobeychik, Y., Letchford, J. & Lakkaraju, K. Data-driven agent-based modeling, with application to rooftop solar adoption. *Auton. Agents Multi-Agent Syst.* **30**, 1023–1049 (2016).
20. Schelling, T. C. Dynamic models of segregation. *J. Math. Sociol.* **1**, 143–186 (1971).
21. Schelling, T. C. Models of segregation. *Am. Econ. Rev.* **59**, 488–493 (1969).
22. Hegselmann, R., Schelling, T. C. & Sakoda, J. M. The intellectual, technical, and social history of a model. *J. Artif. Soc. Soc. Simul.* **20**, 1–10 (2017).
23. Schelling, T. C. *Micromotives and Macrobehavior* (WW Norton & Company, 2006).
24. Fossett, M. & Dietrich, D. R. Effects of city size, shape, and form, and neighborhood size and shape in agent-based models of residential segregation: Are schelling-style preference effects robust?. *Environ. Plan. B* **36**, 149–169 (2009).
25. Fagiolo, G., Valente, M. & Vriend, N. J. Segregation in networks. *J. Econ. Behav. Org.* **64**, 316–336 (2007).
26. Freeman, L. C. Segregation in social networks. *Sociol. Methods Res.* **6**, 411–429 (1978).
27. Henry, A. D., Prałat, P. & Zhang, C.-Q. Emergence of segregation in evolving social networks. *Proc. Natl. Acad. Sci.* **108**, 8605–8610 (2011).
28. Rogers, T. & McKane, A. J. A unified framework for Schelling's model of segregation. *J. Stat. Mech. Theor. Exp.* **2011**, P07006 (2011).
29. Vinković, D. & Kirman, A. A physical analogue of the Schelling model. *Proc. Natl. Acad. Sci.* **103**, 19261–19265 (2006).
30. Scalco, A., Ceschi, A. & Sartori, R. Application of psychological theories in agent-based modeling: The case of the theory of planned behavior. *Nonlinear Dyn. Psychol. Life Sci.* **22**, 15–33 (2018).
31. Wang, G. & Zhang, S. Abm with behavioral bias and applications in simulating China stock market. *J. Artif. Intell. Soft Comput. Res.* **5**, 257–270 (2015).
32. Schrieks, T., Botzen, W. W., Wens, M., Haer, T. & Aerts, J. C. Integrating behavioral theories in agent-based models for agricultural drought risk assessments. *Front. Water* **3**, 686329 (2021).
33. Abella, D., San Miguel, M. & Ramasco, J. J. Aging effects in Schelling segregation model. *Sci. Rep.* **12**, 19376 (2022).
34. Borgonovo, E., Pangallo, M., Rivkin, J., Rizzo, L. & Siggelkow, N. Sensitivity analysis of agent-based models: A new protocol. *Comput. Math. Org. Theory* **28**, 52–94 (2022).
35. Ligmann-Zielinska, A. *et al.* 'One size does not fit all': A roadmap of purpose-driven mixed-method pathways for sensitivity analysis of agent-based models. *J. Artif. Soc. Soc. Simul.* **23**, 1–10 (2020).
36. Niida, A., Hasegawa, T. & Miyano, S. Sensitivity analysis of agent-based simulation utilizing massively parallel computation and interactive data visualization. *PLoS ONE* **14**, e0210678 (2019).
37. Zhang, J. Tipping and residential segregation: A unified Schelling model. *J. Reg. Sci.* **51**, 167–193 (2011).
38. Zhang, J. Residential segregation in an all-integrationist world. *J. Econ. Behav. Org.* **54**, 533–550 (2004).
39. Silver, D., Byrne, U. & Adler, P. Venues and segregation: A revised Schelling model. *PLoS ONE* **16**, e0242611 (2021).
40. Gonzalez, M. C., Hidalgo, C. A. & Barabasi, A.-L. Understanding individual human mobility patterns. *Nature* **453**, 779–782 (2008).
41. Pappalardo, L., Rinzivillo, S., Qu, Z., Pedreschi, D. & Giannotti, F. Understanding the patterns of car travel. *Eur. Phys. J. Spec. Top.* **215**, 61–73 (2013).
42. Pappalardo, L. *et al.* Returners and explorers dichotomy in human mobility. *Nat. Commun.* **6**, 8166 (2015).
43. Barbosa-Filho, H. *et al.* Human mobility: Models and applications. *Phys. Rep.* **734**, 1–74 (2018).
44. Alessandretti, L., Aslak, U. & Lehmann, S. The scales of human mobility. *Nature* **587**, 402–407 (2020).
45. Schläpfer, M. *et al.* The universal visitation law of human mobility. *Nature* **593**, 522–527 (2021).
46. Song, C., Koren, T., Wang, P. & Barabási, A.-L. Modelling the scaling properties of human mobility. *Nat. Phys.* **6**, 818–823 (2010).
47. Simini, F., González, M. C., Maritan, A. & Barabási, A.-L. A universal model for mobility and migration patterns. *Nature* **484**, 96–100 (2012).
48. Simini, F., Barlacchi, G., Luca, M. & Pappalardo, L. A deep gravity model for mobility flows generation. *Nat. Commun.* **12**, 6576 (2021).
49. Hu, T., Luo, J. & Liu, W. Life in the "matrix": Human mobility patterns in the cyber space. In *Proceedings of the International AAAI Conference on Web and Social Media*, vol. 12 (2018).
50. Zhao, Y.-M., Zeng, A., Yan, X.-Y., Wang, W.-X. & Lai, Y.-C. Unified underpinning of human mobility in the real world and cyberspace. *New J. Phys.* **18**, 053025 (2016).
51. Hu, T., Xia, Y. & Luo, J. To return or to explore: Modelling human mobility and dynamics in cyberspace. in *The World Wide Web Conference*, 705–716 (2019).
52. Luca, M., Barlacchi, G., Lepri, B. & Pappalardo, L. A survey on deep learning for human mobility. *ACM Comput. Surv.*https://doi.org/10.1145/3485125 *(2021).*
53. Böhm, M., Nanni, M. & Pappalardo, L. Gross polluters and vehicle emissions reduction. *Nat. Sustain.* **1**, 1–9 (2022).
54. Zipf, G. K. *Human Behavior and the Principle of Least Effort: An Introduction to Human Ecology* (Ravenio Books, 2016).
55. Zipf, G. K. The p 1 p 2/d hypothesis: On the intercity movement of persons. *Am. Sociol. Rev.* **11**, 677–686 (1946).
56. Mauro, G., Luca, M., Longa, A., Lepri, B. & Pappalardo, L. Generating mobility networks with generative adversarial networks. *EPJ Data Sci.* **11**, 58 (2022).
57. Luca, M., Lepri, B., Frias-Martinez, E. & Lutu, A. Modeling international mobility using roaming cell phone traces during covid-19 pandemic. *EPJ Data Sci.* **11**, 22 (2022).
58. Moro, E., Calacci, D., Dong, X. & Pentland, A. Mobility patterns are associated with experienced income segregation in large us cities. *Nat. Commun.* **12**, 4633 (2021).
59. Grauwin, S., Bertin, E., Lemoy, R. & Jensen, P. Competition between collective and individual dynamics. *Proc. Natl. Acad. Sci.* **106**, 20622–20626 (2009).
60. Zipf, G. K. Human behavior and the principle of least effort (1949).
61. Liu, E.-J. & Yan, X.-Y. A universal opportunity model for human mobility. *Sci. Rep.* **10**, 4657 (2020).
62. Prieto Curiel, R., Pappalardo, L., Gabrielli, L. & Bishop, S. R. Gravity and scaling laws of city to city migration. *PLoS ONE* **13**, e0199892 (2018).
63. Lenormand, M., Bassolas, A. & Ramasco, J. J. Systematic comparison of trip distribution laws and models. *J. Transp. Geogr.* **51**, 158–169 (2016).
64. Pappalardo, L., Simini, F., Barlacchi, G. & Pellungrini, R. Scikit-mobility: A Python library for the analysis, generation, and risk assessment of mobility data. *J. Stat. Softw.* **103**, 1–38 (2022).
65. Erlander, S. & Stewart, N. F. *The Gravity Model in Transportation Analysis: Theory and Extensions*, vol. 3 (Vsp, 1990).
66. Karemera, D., Oguledo, V. I. & Davis, B. A gravity model analysis of international migration to North America. *Appl. Econ.* **32**, 1745–1755 (2000).
67. Patuelli, R., Reggiani, A., Gorman, S. P., Nijkamp, P. & Bade, F.-J. Network analysis of commuting flows: A comparative static approach to German data. *Netw. Spat. Econ.* **7**, 315–331 (2007).
68. Balcan, D. *et al.* Modeling the spatial spread of infectious diseases: The global epidemic and mobility computational model. *J. Comput. Sci.* **1**, 132–145 (2010).
69. Li, X., Tian, H., Lai, D. & Zhang, Z. Validation of the gravity model in predicting the global spread of influenza. *Int. J. Environ. Res. Public Health* **8**, 3134–3143 (2011).

70. Cevik, S. Going viral: A gravity model of infectious diseases and tourism flows. *Open Econ. Rev.* **33**, 141–156 (2022).
71. Zhang, Y., Zhang, A. & Wang, J. Exploring the roles of high-speed train, air and coach services in the spread of covid-19 in China. *Transp. Policy* **94**, 34–42 (2020).
72. Louf, R. & Barthelemy, M. Patterns of residential segregation. *PLoS ONE* **11**, e0157476 (2016).
73. Gardner, M. The fantastic combinations of Jhon Conway's new solitaire game' life. *Sci. Am.* **223**, 20–123 (1970).
74. Rinzivillo, S. et al. The purpose of motion: Learning activities from individual mobility networks. in *2014 International Conference on Data Science and Advanced Analytics (DSAA)*, 312–318 (IEEE, 2014).

Acknowledgements

This work has been partially supported by (1) EU project H2020 Humane-AI-net G.A. 952026; (2) EU project H2020 SoBigData++ G.A. 871042; (3) NextGenerationEU—National Recovery and Resilience Plan (Piano Nazionale di Ripresa e Resilienza, PNRR), Project "SoBigData.it—Strengthening the Italian RI for Social Mining and Big Data Analytics", prot. IR0000013, avviso n. 3264 on 28/12/2021. We thank Daniele Fadda for his precious support on data visualization.

Author contributions

G.M. and L.P. conceived and conceptualized the research. D.G. made the simulations, the data analysis, and developed the code. D.G., G.M., and L.P. conceived the figures. D.G. made the plots. G.M., and L.P. wrote the paper. L.P. directed and supervised the research. All authors contributed to the scientific discussion, read and approved the paper.

Competing interests

The authors declare no competing interests.

Additional information

Supplementary Information The online version contains supplementary material available at https://doi.org/10.1038/s41598-023-38519-6.

Correspondence and requests for materials should be addressed to D.G., G.M. or L.P.

Reprints and permissions information is available at www.nature.com/reprints.

Publisher's note Springer Nature remains neutral with regard to jurisdictional claims in published maps and institutional affiliations.